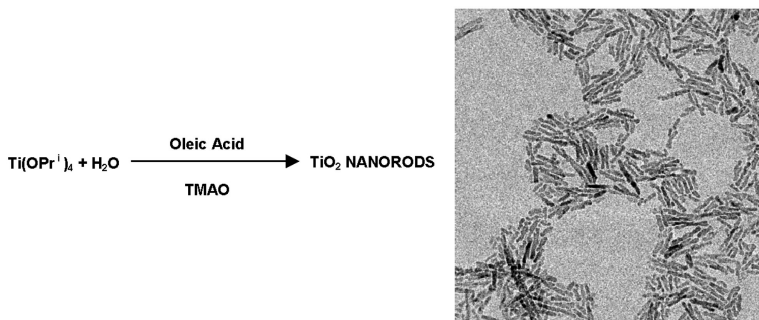


## Low-Temperature Synthesis of Soluble and Processable Organic-Capped Anatase TiO Nanorods

P. Davide Cozzoli, Andreas Kornowski, and Horst Weller

*J. Am. Chem. Soc.*, **2003**, 125 (47), 14539-14548 • DOI: 10.1021/ja036505h • Publication Date (Web): 31 October 2003

Downloaded from <http://pubs.acs.org> on March 30, 2009



### More About This Article

Additional resources and features associated with this article are available within the HTML version:

- Supporting Information
- Links to the 52 articles that cite this article, as of the time of this article download
- Access to high resolution figures
- Links to articles and content related to this article
- Copyright permission to reproduce figures and/or text from this article

[View the Full Text HTML](#)

## Low-Temperature Synthesis of Soluble and Processable Organic-Capped Anatase TiO<sub>2</sub> Nanorods

P. Davide Cozzoli, Andreas Kornowski, and Horst Weller\*

Contribution from the Institute of Physical Chemistry, University of Hamburg,  
Bundesstrasse 45, D-20146 Hamburg, Germany

Received June 4, 2003; E-mail: weller@chemie.uni-hamburg.de

**Abstract:** We demonstrate the controlled growth of high aspect ratio anatase TiO<sub>2</sub> nanorods by hydrolysis of titanium tetraisopropoxide (TTIP) in oleic acid (OLEA) as surfactant at a temperature as low as 80 °C. Chemical modification of TTIP by OLEA is proven to be a rational strategy to tune the reactivity of the precursor toward water. The most influential factors in shape control of the nanoparticles are investigated by simply manipulating their growth kinetics. The presence of tertiary amines or quaternary ammonium hydroxides as catalysts is essential to promote fast crystallization under mild conditions. The novelty of the present approach relies on the large-scale production of organic-capped TiO<sub>2</sub> nanocrystals to which standard processing of colloidal nanocrystals, such as surface ligand exchange, can be applied for the first time. Concentrated colloidal titania dispersions can be prepared for a number of fundamental studies in homogeneous solutions and represent a new source of easily processable oxide material for many technological applications.

### 1. Introduction

One-dimensional (1D) inorganic nanostructures (rods, wires, and tubes) are of both relevant theoretical<sup>1</sup> and technological<sup>2</sup> interest, as they exhibit a wide range of electrical and optical properties that depend on both size and shape.<sup>3</sup> Nevertheless, most efforts of colloidal chemistry have focused on 1D metal<sup>4</sup> or semiconductor<sup>5</sup> nanocrystals, whereas other systems, such as oxides, remain poorly explored.<sup>6,15a-i-1</sup>

Nanocrystalline TiO<sub>2</sub> is one of the most studied oxides, owing to its widespread applications in photocatalysis,<sup>7</sup> solar energy conversion,<sup>8</sup> ductile ceramics,<sup>9</sup> sensors,<sup>10</sup> and mesoporous membranes.<sup>11</sup> The technological potential of titania is expected to be remarkably extended if a fine-tuning of particle morphology is somehow achieved.

In TiO<sub>2</sub>-based photocatalysts,<sup>7a-c</sup> the photogenerated electrons (e<sup>-</sup>) and holes (h<sup>+</sup>) migrate to the nanocrystal surface, where they act as redox sources, ultimately leading to the destruction

of pollutants. In spherical crystals, benefits arising from higher surface-to-volume ratio with decreasing the particle size are significantly offset by the increased e<sup>-</sup>/h<sup>+</sup> recombination probability at surface trapping sites. As a consequence, lower

- (1) (a) Peng, X.; Manna, L.; Yang, W.; Wickham, J.; Scher, E.; Kadavanich, A.; Alivisatos, A. P. *Nature* **2000**, *404*, 59. (b) Hu, J. T.; Li, L. S.; Yang, W. D.; Manna, L.; Wang, L. W.; Alivisatos, A. P. *Science* **2001**, *292*, 2060.
- (2) (a) Colvin, V. L.; Schlamp, M. C.; Alivisatos, A. P. *Nature* **1994**, *370*, 354. (b) Kazes, M.; Lewis, D. Y.; Ebenstein, Y.; Mokari, T.; Banin, U. *Adv. Mater.* **2002**, *14*, 4, 317. (c) Johnson, J. C.; Yan, H.; Schaller, R. D.; Haber, L. H.; Saykally, R. J.; Yang, P. *J. Phys. Chem. B* **2001**, *105*, 46, 11 387. (d) Kind, H.; Yan, H.; Messer, B.; Law, M.; Yang, P. *Adv. Mater.* **2002**, *14*, 2, 158.
- (3) (a) Hu, J.; Odom, T. W.; Lieber, C. M. *Acc. Chem. Res.* **1999**, *32*, 435. (b) Lieber, C. M. *Solid State Comm.* **1998**, *107*, 607–616. (c) Alivisatos, A. P. *Science* **1996**, *271*, 933. (d) Alivisatos, A. P. *J. Phys. Chem.* **1996**, *100*, 13226.
- (4) (a) Sun, Y.; Xia, Y. *Science* **2002**, *298*, 10, 2176. (b) Park, S. J.; Kim, S.; Lee, S.; Khim, Z. G.; Char, K.; Hyeon, T. *J. Am. Chem. Soc.* **2002**, *122*, 8561. (c) Wu, Y.; Yang, P. *Chem. Mater.* **2000**, *12*, 605. (d) Jana, N. R.; Gearheart, L.; Murphy, C. J. *J. Phys. Chem.* **2001**, *105*, 4065. (e) Yu, Y. Y.; Chang, S. S.; Lee, C. L.; Wang, C. R. C. *Phys. Chem. B* **1997**, *101*, 34, 6661. (f) Kim, F.; Song, J. H.; Yang, P. *J. Am. Chem. Soc.* **2002**, *124*, 14316. (g) Corgente, N.; Respaud, M.; Senocq, F.; Casanova, M. J.; Amiens, C.; Chaudret, B. *Nano Lett.* **2001**, *1*, 10, 565.
- (5) (a) Manna, L.; Scher, E. C.; Alivisatos, A. P. *J. Am. Chem. Soc.* **2000**, *122*, 12 700. (b) Manna, L.; Scher, E. C.; Li, L. S.; Alivisatos, A. P. *J. Am. Chem. Soc.* **2002**, *124*, 7136. (c) Zhan, J.; Yang, X.; Wang, D.; Li, S.; Xie, Y.; Xia, Y.; Qiu, Y. *Adv. Mater.* **2002**, *12*, 1348. (d) Lee, S. M.; Jun, Y. W.; Cho, S. N.; Cheon, J. *J. Am. Chem. Soc.* **2002**, *124*, 11 244. (e) Gao, F.; Lu, Q.; Xie, S.; Zhao, D. *Adv. Mater.* **2002**, *14*, 21, 1537. (f) Yang, C. S.; Awschalom, D. D.; Stucky, G. D. *Chem. Mater.* **2002**, *14*, 1277. (g) Chen, C. C.; Chao, C. Y.; Lang, Z. H. *Chem. Mater.* **2000**, *12*, 1516. (h) Kim, Y. H.; Jun, Y. W.; Jun, B. H.; Lee, S. M.; Cheon, J. *J. Am. Chem. Soc.* **2002**, *124*, 13 656. (i) Chen, C. C.; Yeh, C. C. *Adv. Mater.* **2000**, *12*, 738.
- (6) (a) Urban, J. J.; Yun, W. S.; Gu, Q.; Park, H. *J. Am. Chem. Soc.* **2002**, *124*, 7, 1186. (b) Guo, L.; Ji, Y. L.; Xu, H.; Simon, P.; Wu, Z. *J. Am. Chem. Soc.* **2002**, *124*, 14 864. (c) Pacholski, C.; Kornowski, A.; Weller, H. *Angew. Chem., Int. Ed.* **2002**, *41*, 7, 1188. (d) Vayssieres, L.; Beermann, N.; Lindquist, S. E.; Hagfeldt, A. *Chem. Mater.* **2001**, *13*, 2, 233. (e) Pan, Z. W.; Dai, Z. R.; Wang, Z. L. *Science* **2001**, *291*, 1947.
- (7) (a) *Advanced Catalysis and Nanostructured Materials*; Moser, W. R., Ed.; Academic Press: San Diego, 1990. (b) *Photocatalysis and Environment, Trends and Applications*; Schiavello, M., Ed.; Kluwer: Dordrecht, 1988. (c) *Photocatalysis. Fundamentals and Applications*, Pelizzetti, E.; Serpone, N. Eds.; Wiley: New York, 1989. (d) Zhang, Z.; Wang, C. C.; Zakaria, R.; Ying, J. Y. *J. Phys. Chem. B* **1998**, *102*, 10 871. (e) Kominami, H.; Muratami, S.; Kato, J.; Kera, Y.; Ohtani, B. *J. Phys. Chem. B* **2002**, *106*, 10 501.
- (8) (a) O' Regan, B.; Gratzel, M. *Nature* **1991**, *353*, 737. (b) *Photochemical Conversion and Storage of Solar Energy*, Pelizzetti, E.; Serpone, N., Eds.; Kluwer: Dordrecht, 1990. (c) Hagfeldt, A.; Gratzel, M. *Chem. Rev.* **1995**, *95*, 49. (d) Bignozzi, C. A.; Argazzi, R.; Kleverlaan, C. J. *Chem. Soc. Rev.* **2000**, *29*, 87. (e) Nakade, S.; Matsuda, M.; Kambe, S.; Saito, Y.; Kitamura, T.; Sakata, T.; Wada, Y.; Mori, H.; Yanagida, S. *J. Phys. Chem. B* **2002**, *106*, 10004. (f) Nelson, J. *Phys. Rev. B* **1999**, *59*, 23, 15 374. (g) Nelson, J.; Haque, S. A. Klug, D. R.; Durrant, R. J. *Phys. Rev. B* **2001**, *63*, 205–211. (h) Nelson, J. *Curr. Opin. Solid State Mater. Sci.* **2002**, *6*, 87.
- (9) Karch, J.; Birringer, R.; Gleiter, H. *Nature* **1987**, *330*, 556.
- (10) (a) Zhu, Y.; Shi, J.; Zhang, Z.; Zhang, C.; Zhang, X. *Anal. Chem.* **2002**, *74*, 120. (b) Sharma, R. K.; Bhatnagar, M. C.; Sharma, G. L. *Sens. Actuators B: Chem.* **1998**, *46*, 3, 194. (c) Carotta, M. C.; Ferroni, M.; Gnani, D.; Guidi, V.; Merli, M.; Martinelli, G.; Casale, M. C.; Notaro, M. *Sens. Actuators B: Chem.* **1999**, *58*, 1–3, 310. (d) Traversa, E.; Gusmano, G.; Gnappi, G.; Montenero, A. *Sens. Actuators B: Chem.* **1996**, *31*, 1–2, 59.

photocatalytic quantum yields are observed for spherical nanocrystals smaller than a certain dimension (about 10 nm).<sup>7d-e</sup>

On the other hand, in TiO<sub>2</sub>-based dye-sensitized solar cells (DSCs),<sup>8</sup> performances associated with spherical crystals are usually limited by the surface area available for capture of solar light by the adsorbed or anchored dye on the particles, by the distribution and density of surface localized trap states at grain boundaries and by electron percolation pathways in nanocrystallites films.<sup>8e-h</sup>

By comparison, rod-shaped titania nanocrystals could lead to considerable advantages in both technological fields, when compared to nearly spherical particles. In nanorods,<sup>5b</sup> the surface-to-volume ratio is higher than that found in nanospheres, and this would guarantee a high density of active sites available for surface reactions as well as a high interfacial charge carrier transfer rate. Moreover, the increased delocalization of carriers in rods, where they are free to move throughout the length of the crystal, is expected to reduce the e<sup>-</sup>/h<sup>+</sup> recombination probability. This could partially compensate for the occurrence of surface trap states and ensure a more efficient charge separation. Further, nanorods could potentially improve charge transport in photovoltaic devices if densely packed thin films were processed with a controlled orientation of the 1D inorganic electron transporters.<sup>8h</sup>

Currently developed methods to one-dimensional TiO<sub>2</sub> crystals mainly comprise sol-gel template,<sup>12</sup> surfactant-directed<sup>13</sup> and hydrothermal methods.<sup>14</sup> Unfortunately, these routes typically provide insoluble wire- and tubular-like TiO<sub>2</sub> structures which are a few hundred nanometers to microns in length, and which range from a few tens to several tens of nanometers in diameter.

On the other hand, although wet-chemistry<sup>15-18</sup> synthetic efforts to crystalline TiO<sub>2</sub> have been even more numerous, preparative routes to unidirectional TiO<sub>2</sub> crystals in the nanosized regime need to be further developed and rationalized. The

formation of rodlike rutile TiO<sub>2</sub> nanocrystals has been observed in acidic media upon hydrothermal treatments,<sup>15m,18c-e</sup> although with the coexistence of anatase and/or brookite traces in some cases. The fine-tuning of TiO<sub>2</sub> nanoparticles morphology in the exclusive anatase phase has been even more rarely documented. Only a few works have focused on the preparation of shape-controlled titania particles. Triangular-like or elongated nanocrystals from self-assembled clusters,<sup>15a</sup> pseudocubic or ellipsoidal particles<sup>15i-1</sup> with varying aspect ratios (8–100 nm in diameter and 20–200 nm in length) have been synthesized by means of organic shape-controllers in aqueous media.

The requirement of high crystallinity is, in fact, a major problem in TiO<sub>2</sub> synthesis. Sol-gel preparations (based on both hydrolytic<sup>15</sup> and non-hydrolytic<sup>16</sup> reaction pathways) and microemulsions<sup>17a-b</sup> typically provide amorphous titanium dioxide. Calcination of gels or thermal annealing<sup>17c-e</sup> of microemulsions are therefore required to induce crystallization of the nanoparticles, although leading to phase transformation, sintering, grain growth, and loss of surface area in many cases. Hydrothermal synthesis<sup>14,18</sup> are directly carried out at high temperatures, but the resulting nanocrystals are rather agglomerate, insoluble in most solvents and show chemical and physical properties strongly depending on the reaction conditions. The role of precursors, additives, catalysts, pH, and solvent in determining the degree of crystallization, crystal phase composition, and morphologies have been emphasized and discussed on the basis of coordination chemistry.<sup>15-18</sup> Stabilizing agents have been used to prevent agglomeration, but, with a few exceptions,<sup>15a</sup> particles are crystalline after a long (3 days) or short (from 5 min to a few hours) aging at moderate (140 °C)<sup>15i-1</sup> or high temperatures (250–300 °C),<sup>16f,17c</sup> respectively. Recently, the growth of nearly spherical anatase TiO<sub>2</sub> nanoparticles has been demonstrated even at 40 °C by means of a time-consuming (7–14 d) nonaqueous procedure.<sup>16d-e</sup>

In this scenario, the search for one-step, low-temperature routes to well-crystallized anatase titania nanoparticles of controlled size and shape<sup>15a,15i-1</sup> is still an open challenge. Moreover, solubility of TiO<sub>2</sub> nanocrystals is required to enable the study of their fundamental optical and catalytic properties under solution-like conditions, as well as to provide precursors for realizing devices. To date, standard procedures known from colloidal chemistry, such as re-dispersion of nanocrystals in optically clear organic solutions after extraction from the reaction bath and surface ligand exchange, have not been reported for TiO<sub>2</sub>. The possibility of both dispersing a techno-

- (11) (a) Bischoff, B. L.; Anderson, M. A. *Chem. Mater.* **1995**, *7*, 1772. (b) Yin, J. B.; Zhao, X. P. *Chem. Mater.* **2002**, *14*, 4633. (c) Sibū, C. P.; Kumar, S. R.; Mukundan, P.; Warrior, K. G. K. *Chem. Mater.* **2002**, *14*, 2876.
- (12) (a) Martin, C. R. *Science* **1994**, *266*, 1961. (b) Hulteen, J. C.; Martin, C. R. *J. Mater. Chem.* **1997**, *7* (7), 1075. (c) Lakshmi, B. B.; Dorhout, P. K.; Martin, C. R. *Chem. Mater.* **1997**, *9*, 857. (d) Hulteen, J. C.; Martin, C. R. *J. Mater. Chem.* **1997**, *7* (7), 1075. (e) Limmer, S. J.; Seraji, S.; Forbess, M. J.; Wu, Y.; Chou, T. P.; Nguyen, C.; Cao, G. *Adv. Mater.* **2001**, *16*, 1269. (f) Matsui, K.; Kyotani, T.; Tomita, A. *Adv. Mater.* **2002**, *14*, 1216. (g) Imai, H.; Takei, Y.; Shimizu, K.; Matsuda, M.; Hirashima, H. *J. Mater. Chem.* **1999**, *9*, 2971. (h) Hoyer, P. *Langmuir* **1996**, *12*, 1411. (i) Miao, Z.; Xu, D.; Ouyang, J.; Guo, G.; Zhao, X.; Tang, Y. *Nano Lett.* **2002**, *2*, 717. (l) Kasuga, T.; Hiramatsu, M.; Hoson, A.; Sekino, Niihara, K. *Adv. Mater.* **1999**, *11*, 1307.
- (13) (a) Muhr, H. J.; Krumeich, F.; Schonholzer, U. P.; Bieri, F.; Niederberger, M.; Gauckler, L. J.; Nesper, R. *Adv. Mater.* **2000**, *12*, 231. (b) Yada, M.; Mihara, M.; Mouri, M.; Kuroki, M.; Kijima, T. *Adv. Mater.* **2002**, *14*, 309. (c) Yang, P.; Zhao, D.; Margolese, D. I.; Chmelka, B. F.; Stucky, G. D. *Chem. Mater.* **1999**, *11*, 2813.
- (14) (a) Li, Y.; Sui, M.; Ding, Y.; Zhang, G.; Zhuang, J.; Wang, C. *Adv. Mater.* **2000**, *12*, 818. (b) Chen, Q.; Zhou, W.; Du, G.; Peng, L. M. *Adv. Mater.* **2002**, *14*, 1208. (c) Lou, X. W.; Zeng, H. C. *Chem. Mater.* **2002**, *14*, 4781–4789. (d) Gui, Z.; Fan, R.; Mo, W.; Chen, X.; Yang, L.; Zhang, S.; Hu, Y.; Wang, Z.; Fan, W. *Chem. Mater.* **2002**, *14*, 5053.
- (15) (a) Chemseddine, A.; Moritz, A. *Eur. J. Inorg. Chem.* **1999**, 235. (b) Bischoff, B. L.; Anderson, M. A. *Chem. Mater.* **1995**, *7*, 2. (c) Murakami, Y.; Matsumoto, T.; Takasu, Y. *J. Phys. Chem. B* **1999**, *103*, 1836. (d) Poznyak, S. K.; Talapin, D. V.; Kulak, A. I. *J. Phys. Chem. B* **2001**, *105*, 4816. (e) Lopez, T.; Hernandez, J.; Gomezs, R.; Bokhimi, X.; Boldu, J. L.; Munoz, E.; Novaro; Garcia-Ruiz, A. *Langmuir* **1999**, *15*, 5689. (f) Bokhimi, X.; Boldu, J. L.; Hernandez, J.; Gomez, R.; Garcia-Ruiz, A. *Chem. Mater.* **1999**, *11*, 2716. (g) Colomer, M. T.; Jurado, J. R. *Chem. Mater.* **2000**, *12*, 923–930. (h) O'Brien, S.; Brus, L.; Murray, C. B. *J. Am. Chem. Soc.* **2001**, *123*, 12085. (i) Sugimoto, T.; Zhou, X.; Muramatsu, A. *J. Colloid Interface Sci.* **2003**, *259*, 43. (l) Sugimoto, T.; Zhou, X.; Muramatsu, A. *J. Colloid Interface Sci.* **2003**, *259*, 53. (m) Zhang, Q.; Gao, L. *Langmuir* **2003**, *19*, 967.
- (16) (a) Hay, J. N.; Raval, H. M. *Chem. Mater.* **2001**, *13*, 3396. (b) Vioux, A. *Chem. Mater.* **1997**, *9*, 2292. (c) Arnal, P.; Corriu, R. J. P.; Leclercq, D.; Mutin, P. H.; Vioux, A. *Chem. Mater.* **1997**, *9*, 694. (d) Niederberger, M.; Bartl, M. H.; Stucky, G. *Chem. Mater.* **2002**, *14*, 4364. (e) Niederberger, M.; Bartl, M. H.; Stucky, G. D. *J. Am. Chem. Soc.* **2002**, *124*, 13642. (f) Trentler, T. J.; Denler, T. E.; Bertone, J. F.; Agrwal, A.; Colvin, V. L. *J. Am. Chem. Soc.* **1999**, *121*, 1613.
- (17) (a) Papoutsis, D.; Lianos, P.; Yianoulis, P.; Koutsoukos, P. *Langmuir* **1994**, *10*, 1684. (b) Stathatos, E.; Lianos, P.; Del Monte, F.; Levy, D.; Tsiourvas, D. *Langmuir* **1997**, *13*, 4295. (c) Lin, J.; Lin, Y.; Liu, P.; Mezziani, J. M.; Allard, L. F.; Sun, Y. P. *J. Am. Chem. Soc.* **2002**, *124*, 11 514. (d) Andersson, M.; Osterlund, L.; Ljungstrom, S.; Palmqvist, A. *J. Phys. Chem. B* **2002**, *106*, 10674. (e) Wu, M.; Long, J.; Huang, A.; Luo, Y.; Feng, S.; Xu, R. *Langmuir* **1999**, *15*, 8822.
- (18) (a) Ovenstone, J.; Yanagisawa, K. *Chem. Mater.* **1999**, *11*, 2770. (b) Wang, C. C.; Ying, J. Y. *Chem. Mater.* **1999**, *11*, 3113. (c) Cheng, H.; Ma, J.; Zhao, Z.; Qi, Z. *Chem. Mater.* **1995**, *7*, 663. (d) Wu, M.; Lin, G.; Wang, G.; He, D.; Feng, S.; Xu, R. *Chem. Mater.* **2002**, *14*, 1974. (e) Wang, C.; Deng, Z. X.; Li, Y. *Inorg. Chem.* **2001**, *40*, 5210. (f) Komimami, H.; Kohno, M.; Takada, Y.; Inoue, M.; Inui, T.; Kera, Y. *Ind. Eng. Chem. Res.* **1999**, *38*, 3925. (g) Yanagisawa, K.; Ovenstone, J. *J. Phys. Chem. B* **1999**, *103*, 7781. (h) Wang, C. C.; Ying, J. Y. *Chem. Mater.* **1999**, *11*, 3113.

logically valuable nanosized material into different media and of providing some control over its surface by passivation of surface traps and by surface functionalization through the attachment of different organic ligands represents a major goal in nanocrystal chemistry.

In this paper, we demonstrate the controlled growth of anatase TiO<sub>2</sub> nanorods at low temperatures (80–100 °C) with oleic acid as surfactant. Hydrolysis of a titanium alkoxide has been employed and manipulated by means of a strategy, relying on the chemical modification of the titanium precursor by the carboxylic acid, and on the use of suitable catalysts (tertiary amines or quaternary ammonium hydroxides) to promote fast (in 4–6 h) crystallization in mild conditions. The factors affecting the morphology of the nanoparticles (from rods to nearly spherical) have been investigated by manipulating their growth kinetics. The obtained titania nanocrystals can be dispersed in optically clear concentrated solutions because of their oleic acid surface coating. This latter can be easily exchanged with stronger ligands (such as phosphonic acids), providing solutions with excellent stability over months and that may be regarded as a new source of easily processable oxide material for technological applications.

## 2. Experimental Section

**2.1 Materials.** All chemicals were of the highest purity available and were used as received without further purification. Titanium tetraisopropoxide (Ti(OPr<sup>i</sup>)<sub>4</sub> or TTIP, 99.999%), trimethylamino-*N*-oxide dihydrate or anhydrous ((CH<sub>3</sub>)<sub>3</sub>NO or TMAO, 98%), trimethylamine ((CH<sub>3</sub>)<sub>3</sub>N or TMA, water solution), tetramethylammonium hydroxide ((CH<sub>3</sub>)<sub>4</sub>NOH or TMAH, water solution), tetrabutylammonium hydroxide ((C<sub>4</sub>H<sub>9</sub>)<sub>4</sub>NOH or TBAH, water solution), anhydrous ethyleneglycol (HO(CH<sub>2</sub>)<sub>2</sub>OH or EG, 99.8%), heptadecane (C<sub>17</sub>H<sub>36</sub> or HPD, 99%), and oleic acid (C<sub>18</sub>H<sub>33</sub>CO<sub>2</sub>H or OLEA, 90%) were purchased from Aldrich. Hexadecane (C<sub>16</sub>H<sub>34</sub> or HXD, 98%), triethylamine ((C<sub>2</sub>H<sub>5</sub>)<sub>3</sub>N or TEA, 99.5%) and tributylamine ((C<sub>4</sub>H<sub>9</sub>)<sub>3</sub>N or TBA, 99%) were purchased from Fluka. *n*-octyl-(C<sub>8</sub>H<sub>17</sub>PO(OH)<sub>2</sub> or OPA, 98%) and *n*-tetradecyl-(C<sub>14</sub>H<sub>29</sub>PO(OH)<sub>2</sub> or TDPA, 98%) phosphonic acids were purchased from Alfa Aesar.

All solvents used were of analytical grade and purchased from Aldrich.

**2.2. Synthesis of TiO<sub>2</sub> Nanoparticles.** Two different methods were applied to the synthesis of TiO<sub>2</sub> nanocrystals.

**Fast Hydrolysis Method.** TiO<sub>2</sub> nanorods were obtained by this method. All manipulations were performed using the standard Schlenk technique. In a typical synthesis, 35 g of oleic acid (OLEA) was dried at 120 °C for 1 h under vigorous stirring in a 50 mL three-neck flask connected to a reflux cooler, after which it was cooled to 80–100 °C under nitrogen flow. 1–10 mmol of TTIP was then added and allowed to stir for 5 min: the solution turned from colorless to pale yellow, indicating the formation of a complex. The absence of water at this stage prevented the premature hydrolysis of the molecular precursor. A 0.5–5 mL of a 0.1–2 M aqueous base solution (TMAO, TMA, TMAH, or TBAH) was loaded into a 5 mL syringe and then rapidly injected. When water-insoluble bases (TEA and TBA) were employed as catalysts, they were added to the TTIP/OLEA mixture before water injection. Upon injection, the temperature dropped to about 75–90 °C, after which it was again heated to the initial injection temperature in a few minutes. At this point, the mixture appeared only slightly turbid. A remarkable increase in the solution viscosity slowly occurred in 60–90 min, depending on precursor concentration and on the amount of injected water. The solution was maintained in a closed system at 80–100 °C and stirred under mild reflux with water over 6–12 h to promote further hydrolysis and crystallization of the product. The reaction was

stopped by removing the heat source. Finally, upon carefully removing the remaining water content under vacuum, the turbid reaction mixture turned clear.

**Slow Hydrolysis Method.** Nearly spherical TiO<sub>2</sub> nanocrystals were obtained by this method. In a typical synthesis, 2–10 mmol of TTIP was added to 35 g of degassed OLEA under nitrogen flow at 100 °C and allowed to stir for 5 min, giving a pale yellow solution. A 4–10 mmol of a base (anhydrous TMAO, TEA, or TBA) in 3.2–6.4 g (50–100 mmol) of ethyleneglycol (EG) was subsequently added. The solution was maintained in a close system and stirred at 100 °C over 48 h. The reaction mixture appeared clear during the whole period of the particle growth. Hydrolysis of the titanium precursor was believed to occur upon reaction with water released slowly upon esterification of OLEA and EG. No precipitate could be, in fact, obtained without any alcohol added in the OLEA/TTIP mixture.

**Extraction Procedures.** The extraction procedures were subsequently performed in air: TiO<sub>2</sub> nanocrystals were readily precipitated upon addition of an excess of ethanol (or methanol) to the reaction mixture at room temperature. The resulting precipitate was isolated by centrifugation and washed twice with ethanol to remove surfactant residuals. The OLEA-coated TiO<sub>2</sub> nanoparticles were then easily re-dispersed in solvents such as chloroform or hexane, without any further growth or irreversible aggregation. If washing of the precipitate was repeated several times, then the nanoparticles generally resulted in being insoluble in apolar solvents. Upon small addition of fresh OLEA (some drops of a 0.1 M solution in CHCl<sub>3</sub>), complete solubility could be recovered. The as-obtained TiO<sub>2</sub> nanocrystal solutions were stable for a few weeks, after which some precipitation of titania was observed, depending on the initial nanocrystal concentration.

The TiO<sub>2</sub> powders for XRD and FTIR analysis were prepared by washing the extracted precipitate repeatedly in order to remove physisorbed surfactant molecules, and then evaporating the residual solvent under vacuum at room temperature.

**Surface Ligand Exchange.** The OLEA coating on TiO<sub>2</sub> nanoparticles could be easily exchanged by capping with an alkylphosphonic acid by the following procedure. First, the as-prepared TiO<sub>2</sub> nanocrystals were repeatedly (at least 6 times) washed. At this point, we considered that most capping OLEA had been removed from the nanocrystal surface as they had lost solubility. A volume of 3–4 mL of CHCl<sub>3</sub> was then added to the precipitate to prepare a turbid suspension. An OPA or TDPA 0.2 M solution in CHCl<sub>3</sub> was subsequently dropped under stirring at R. T. until a clear solution was obtained. The resulting mixture was allowed to stir at room temperature for 90 min, after which methanol was added to precipitate the nanoparticles again. The nanoparticles were then washed repeatedly and easily redispersed in CHCl<sub>3</sub> or hexane. By this treatment, exceptionally concentrated transparent solution could be obtained (1–2 mmol of TiO<sub>2</sub>/mL), that were stable over months without further addition of phosphonic acid molecules.

Notably, whereas OLEA could be removed and subsequently reattached onto the TiO<sub>2</sub> surface upon several cycles of nanocrystal washing/OLEA addition as described above, reverse exchange of phosphonic acids with OLEA could not be carried out. The either OPA- or TDPA-capped nanocrystals, in fact, retained their solubility even after repeated washing, thus still indicating the presence of unremoved phosphonic ligands on their surface.

**2.3. Characterization of Samples. UV–Vis Absorption Spectroscopy.** Absorption spectra were measured using an using a Cary 3 (Varian) spectrophotometer.

**Infrared Spectroscopy.** FT-IR spectra of TiO<sub>2</sub> powders before and after ligand exchange procedures were collected with a Bruker Equinox 55 Spectrometer with a resolution of 4 cm<sup>-1</sup>. Measurements were performed with pressed pellets which were made using KBr powder as diluent.

**Powder X-ray Diffraction.** XRD patterns of TiO<sub>2</sub> nanocrystal powders were collected with a Philips X'Pert diffractometer in Bragg–

Brentano reflection geometry using filtered Cu K $\alpha$  radiation ( $\lambda = 1.54056 \text{ \AA}$ ). For XRD measurements the nanocrystal powder was placed on a silicon sample holder.

**Transmission Electron Microscopy.** Transmission electron microscopy (TEM) and high-resolution TEM (HRTEM) images were obtained using a Philips CM-300 UT microscope (TEM) operating at 300 kV. The samples were prepared by dropping dilute solutions of isolated TiO<sub>2</sub> nanoparticles in chloroform onto 400-mesh carbon-coated copper grids and immediately evaporating the solvent. The samples were stable under the electron beam and did not degrade within the typical observation time.

### 3. Results

In this work, organic-capped anatase TiO<sub>2</sub> nanorods were synthesized by hydrolysis of titanium tetraisopropoxide (TTIP) using technical oleic acid (OLEA) as surfactant at low temperatures (80–100 °C). Hydrolysis of TTIP was carried out by an excess of aqueous base solution with respect to TTIP (H<sub>2</sub>O:TTIP molar ratio ranging from 40:1 to 150:1). Tertiary amines or quaternary ammonium hydroxides were employed as catalysts for polycondensation in order to ensure a crystalline product (see Discussion). The influence of the synthesis conditions on the morphology of the resulting TiO<sub>2</sub> nanocrystals was investigated by varying two fundamental parameters: the modality of water supply and the oleic acid (OLEA) content in the growing mixture.

**3.1. Synthesis of TiO<sub>2</sub> Nanorods in Pure Oleic Acid.** TiO<sub>2</sub> nanorods were obtained when the aqueous base solution was rapidly injected in a single portion into OLEA:TTIP mixtures (fast hydrolysis method). The OLEA:TTIP molar ratio was typically in the range 15:1–130:1. As a matter of fact, TiO<sub>2</sub> growth kinetics in OLEA exhibited some unique features. No precipitate (either amorphous or crystalline) could be recovered at  $T < 80 \text{ °C}$ , even after long reaction times (up to one week). Only a slightly turbidity of the reaction mixture was observed and ascribed to incomplete solubilization of water in OLEA under reverse micelle conditions. By contrast, at temperatures higher than this threshold (up to 100 °C), an increase in solution viscosity slowly occurred after addition of the aqueous base. This fact indicated that hydrolysis of TTIP proceeded, thus leading to gelification of the mixture.

The growth kinetics of the TiO<sub>2</sub> nanorods was followed by monitoring the crystallization process of the particles at various reaction times. Representative XRD patterns of samples extracted from the same reaction bath at different times from injection are shown in Figure 1. The reported data refer to a typical TTIP hydrolysis reaction in the presence of TMAO as base catalyst. The XRD profile of fully grown TiO<sub>2</sub> nanorods (Figure 1d) can coincidentally be indexed by the known standard TiO<sub>2</sub> anatase pattern (Figure 1a). Notably, the characteristic line broadening of diffraction peaks points to nanosized crystalline domain. In contrast to the standard pattern, the XRD profile of the TiO<sub>2</sub> sample in Figure 1d clearly exhibits an extreme peak intensity and narrow width for the  $\langle 004 \rangle$  reflex and a comparatively lower diffraction intensity for the  $\langle 200 \rangle$ ,  $\langle 211 \rangle$ , and  $\langle 220 \rangle$  reflexes. Such features imply the formation of rodlike nanocrystals with a preferred growth orientation along the  $c$ -axis of the anatase lattice.

The temporal behavior in Figure 1 evidenced that crystalline domains could be clearly detected within a hour (Figure 1c) after injection of aqueous base and that anisotropic growth

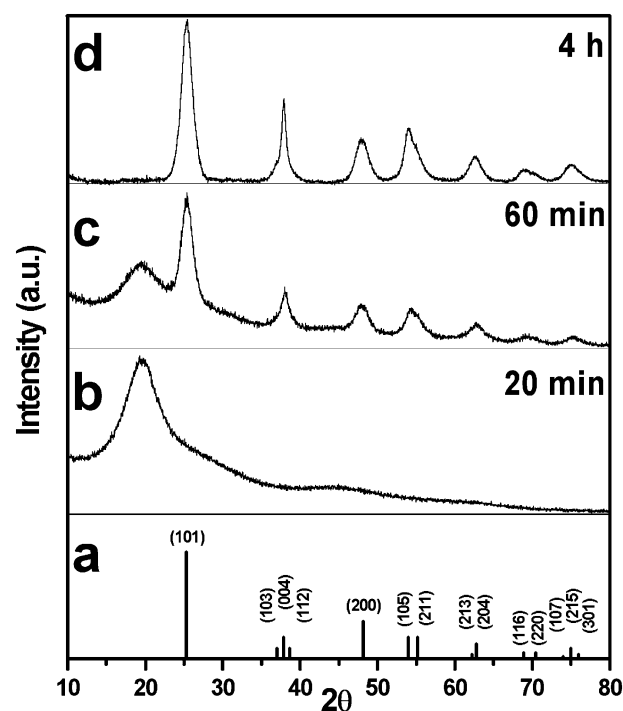


**Figure 1.** XRD pattern of TiO<sub>2</sub> nanocrystals prepared by the fast hydrolysis method (OLEA 35 g, TTIP 5 mmol, TMAO 2M 5 mL) and extracted at different reaction times (b–d) after the aqueous base injection. The standard TiO<sub>2</sub> anatase diffraction lines (a) are also reported.

proceeded rapidly. In addition, the average length of the short axis (according to the fwhm of the  $\langle 101 \rangle$  reflex) increased more slowly in time. The presence of amorphous material (partially condensed hydrous titanium dioxide) was put into relation with the pronounced background at low  $2\theta$  values in the XRD pattern, resulting in a large reflex centered on about  $2\theta = 20^\circ$  (Figure 1b–c). The intensity of this feature was, in fact, comparable to that of anatase peaks at the early stages of growth and progressively decreased with the reaction proceeding to completion. Full crystallization and consumption of titanium precursor could be obtained in just a few hours (4–6 h) at 80–100 °C, whereas prolonged heating did not further influence the particle growth.

As a confirmation of XRD analysis, Figure 2a shows a typical TEM image of nanorods corresponding to Figure 1d. The picture shows that the sample consists of high aspect ratio individual particles, having uniform lengths up to 40 nm and diameter of 3–4 nm. The nanorods appear rather well spaced on the grid, because of the OLEA coating. HRTEM shows (Figure 2d) the single crystal nature of such nanorods, being nearly perfect anatase with an extended crystalline domain in the  $c$ -axis direction (Figure 2g). Samples at earlier growth stages could not be investigated by TEM as they contained a relevant fraction of amorphous material.

By applying the fast hydrolysis method, TiO<sub>2</sub> nanorods were thus grown, which exhibited similar structural and morphological features regardless of growth temperature. By decreasing TTIP concentration and the volume of the aqueous base, rods of lower aspect ratio (shorter in length and larger in diameter) were detected (data not shown). Even if some crystalline product could be obtained without any catalyst added, a base:TTIP molar ratio of 2–4 was found optimal in order to minimize crystallization times and make the reaction proceed to comple-

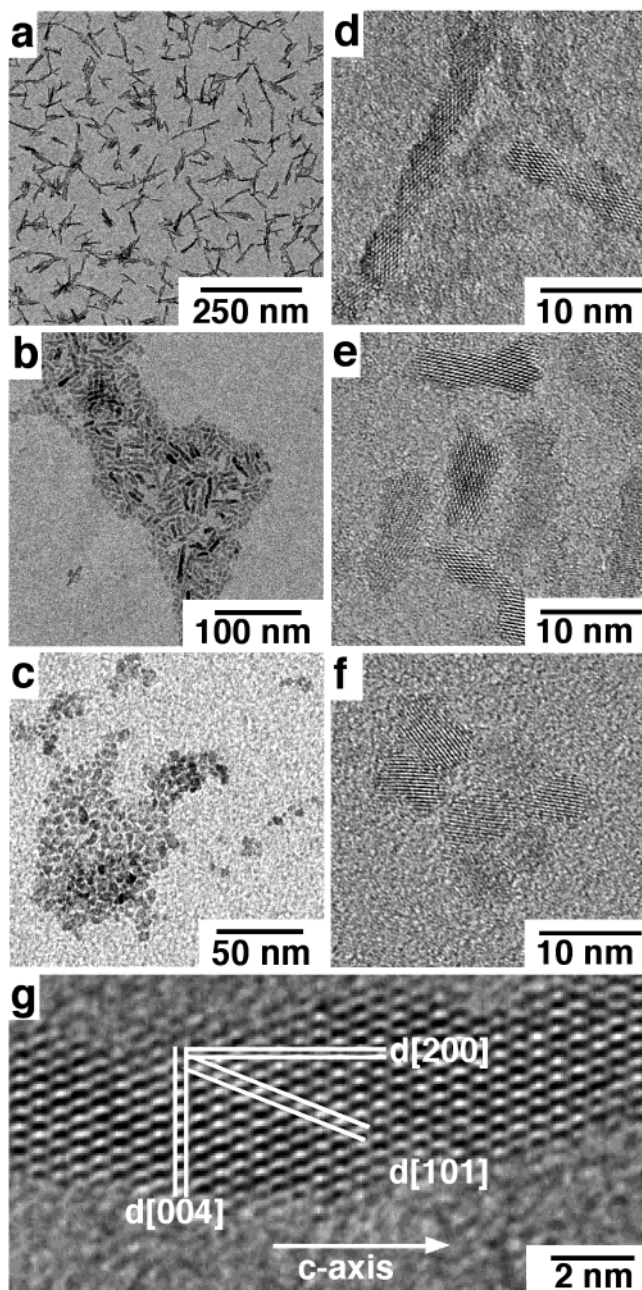


**Figure 2.** TEM overview of TiO<sub>2</sub> nanocrystals prepared in different conditions by the fast (a and b) and by the slow (c) hydrolysis method at 100 °C: (a) OLEA 35 g, TTIP 5 mmol, TMAO 2M 5 mL; (b) OLEA 35 g, TTIP 1 mmol, TBAH 10 mmol, H<sub>2</sub>O 2 mL; (c) OLEA 35 g, EG 3.2 g, TTIP 1 mmol, TMAO 4 mmol. The HRTEM images of the same samples are shown in (d), (e), and (f), respectively. (g) High magnification picture of a single nanorod showing the growth orientation by identification of the anatase lattice planes.

tion. The use of bulky base catalysts (such as TBAH) at a base: TTIP ratio higher than 4 led to an increased length polydispersity (see Figure 2b and the corresponding HRTEM in Figure 2e).

**3.2. Synthesis of TiO<sub>2</sub> Nanocrystals in Oleic Acid/Alkane Mixtures.** To understand the role of OLEA in the growth mechanism, we systematically decreased the relative content of the surfactant in the growing mixtures by progressive substitution of OLEA with a noncoordinating solvent, such as heptadecane or hexadecane, while keeping all other preparative conditions constant. The typical XRD patterns of powders

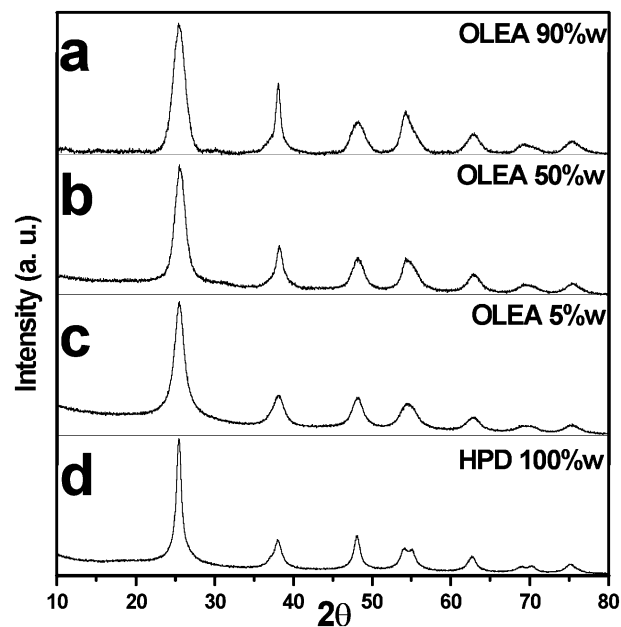


**Figure 3.** XRD diffraction patterns of TiO<sub>2</sub> samples prepared by the fast hydrolysis method in different OLEA:HPD mixtures (growing mixture 35 g, TTIP 1 mmol, TMAO 2M 2 mL injected).

synthesized by the fast hydrolysis method in various OLEA/alkane mixtures are shown in Figure 3.

It is apparent that unidirectional growth is progressively suppressed with decreasing OLEA/alkane ratio. At a limiting OLEA content around 5 wt%, an XRD pattern corresponding to nearly spherical nanoparticles was measured (Figure 3c). TEM investigations (data not shown) revealed that samples at intermediate compositions consisted of a mixture of nearly spherical particles and rods of various lengths. However, reduction of OLEA content in the growing mixtures led to two additional consequences. First, the time required for complete crystallization drastically increased from a few hours (for reactions in pure OLEA) to 48 h (in absence of OLEA). Second, aggregation between particles was prone to occur in the reaction vessel, ultimately leading to insoluble precipitates. In absence of surfactant, bigger crystalline domains were detected (Figure 3d).

**3.3. Synthesis of Spherical TiO<sub>2</sub> Nanocrystals.** To investigate the role of H<sub>2</sub>O in the TiO<sub>2</sub> growth mechanism in pure OLEA, experiments were carried out in which water was slowly released in situ upon esterification of OLEA with ethyleneglycol (EG) (slow hydrolysis method). Complete hydrolysis-polycondensation of TTIP required 48–60 h by this procedure, as the esterification rate is likely the bottleneck of the overall reaction rate. The amount of EG was adjusted to ensure a final production of water in excess with respect to TTIP, as in the case of the fast hydrolysis method. Bases probably acted as catalysts for both OLEA-EG esterification and polycondensation of Ti–O–Ti inorganic network. The measured XRD pattern is similar to that of nearly spherical TiO<sub>2</sub> anatase particles in Figure 3c. The TEM image in Figure 2c confirms that the sample typically consisted of nearly spherical or slightly elongated particles (see the HRTEM in Figure 2f). Reactions performed by the fast injection technique in identical OLEA:EG:TTIP mixtures again provided rods with characteristics similar to those obtained without EG, thus excluding that EG itself affected particles morphologies to some extent. The shape of the resulting particles

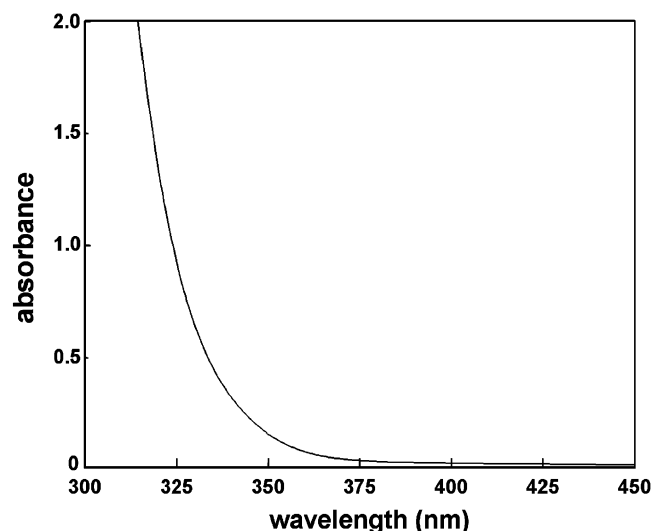


**Figure 4.** Typical UV-vis absorption spectrum of dilute ( $[\text{TiO}_2] \approx 0.005 \text{ M}$ )  $\text{CHCl}_3$  solutions of OLEA-coated  $\text{TiO}_2$  nanocrystals. Titania rodlike and spherical particles show identical absorption features.

was therefore considered to be related to the modality of water supply in the reaction mixture, as other reaction parameters were unchanged with respect to those of the fast injection method.

**3.4. Postsynthesis Processing.** The as prepared  $\text{TiO}_2$  nanorods or nanospheres could remain dispersed in their OLEA mother solution for months without precipitation. After isolation from the reaction medium and removal of excess surfactant upon washing, they were highly soluble in  $\text{CHCl}_3$  or hexane (up to 1 mmol  $\text{TiO}_2/\text{mL}$ ). The color of the solution ranged from transparent to dark yellow, depending on  $\text{TiO}_2$  concentration. Nevertheless, premature precipitation was observed after 10–15 d of storage at RT. This drawback could be eliminated upon addition (1–2 drops/mL) of fresh OLEA (thus ensuring a little excess of surfactant in the solution) or by exchanging the OLEA ligands on the nanocrystal surface with long-chain phosphonic acids. OPA- and TDPA-capped  $\text{TiO}_2$  nanocrystals provided organic solutions of nanorods which were exceptionally stable over several months. The typical unstructured UV-vis absorption spectrum of  $\text{TiO}_2$  nanoparticles is shown in Figure 4.

**3.5.  $\text{TiO}_2$  Surface Characterization: Ligand Exchange.** The nature of the organic coating on the surface of the  $\text{TiO}_2$  nanocrystals was investigated by FT-IR spectroscopy and interpreted on the basis of previously reported studies on the anchoring of phosphonic acids<sup>21</sup> and oleic acid<sup>22</sup> onto the surface of titania.

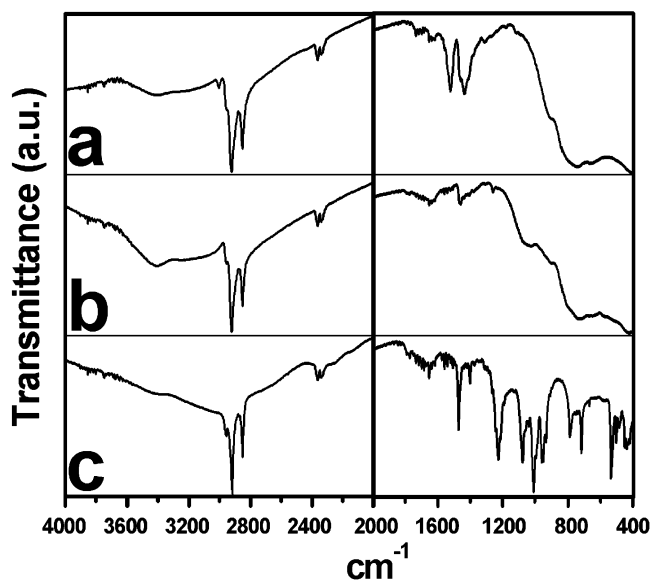


**Figure 5.** FT-IR spectra in the  $4000\text{--}400 \text{ cm}^{-1}$  region of: (a) as-prepared OLEA-capped  $\text{TiO}_2$  nanorods (b) after surface modification with TDPA; (c) TDPA. The spectral region below  $2000 \text{ cm}^{-1}$  has been rescaled for sake of clarity.

In Figure 5 the typical IR spectra in the region  $4000\text{--}400 \text{ cm}^{-1}$  of a  $\text{TiO}_2$  nanorod sample before and after surface modification with an alkylphosphonic acid (TDPA) are presented. The spectrum of pure TDPA is also shown for a comparison.

Above  $2000 \text{ cm}^{-1}$ , both  $\text{TiO}_2$  samples (Figure 5a–b) exhibit the intense antisymmetric and symmetric C–H stretching vibrations<sup>22</sup> (at  $2920$  and  $2850 \text{ cm}^{-1}$ , respectively) of the  $-\text{CH}_2-$  groups in the hydrocarbon moiety. The shoulder at  $2960 \text{ cm}^{-1}$  can be associated with the asymmetric stretching of the terminal  $-\text{CH}_3$  group of the alkyl chain. Notably, in the OLEA-capped  $\text{TiO}_2$  sample (Figure 5a) a weak but definite band at  $3008 \text{ cm}^{-1}$  is also present, attributable to the olefinic C–H stretching.<sup>22b</sup> Such a band is absent in the TDPA-capped  $\text{TiO}_2$  sample (Figure 5b). In addition, the C–H stretching signals in the  $\text{TiO}_2$  samples are superimposed on an underlying surface O–H (from titanol groups or adsorbed  $\text{H}_2\text{O}$ ) broad stretching band centered at  $3300 \text{ cm}^{-1}$ . (In the spectrum of pure TDPA (Figure 5c), the C–H bands are overlapped with a O–H band which is remarkably shifted to shorter wavenumbers ( $3000 \text{ cm}^{-1}$ ) likely because of the involvement of phosphonic headgroups in strong H-bondings.)

Below  $2000 \text{ cm}^{-1}$ , the  $\text{COO}^-$  antisymmetric and symmetric stretching vibrations (two characteristic bands centered at  $1520$  and  $1436 \text{ cm}^{-1}$ , respectively) of carboxylate anions<sup>22</sup> complexed with surface Ti centers dominate in the spectra of the OLEA-capped  $\text{TiO}_2$  nanocrystals (Figure 5a). From the value of their frequency difference ( $\Delta\nu \approx 84 \text{ cm}^{-1}$ ), the mode of binding of carboxylate adsorbates onto the  $\text{TiO}_2$  surface might be interpreted as being chelating bidentate.<sup>22b,22d</sup> The lack of clear evidence for the free C=O stretching band at around  $1650\text{--}1720 \text{ cm}^{-1}$  (cf.  $1775 \text{ cm}^{-1}$  for OLEA in the vapor phase) seems to exclude the presence of both un-ionized OLEA monomers and dimers<sup>22b–c</sup> possibly having the C=O involved in H-bonding with a  $\text{Ti}-\text{OH}_2^+$  surface group. It deserves to be noticed that the characteristic  $\text{COO}^-$  bands are not observable in the spectrum of the  $\text{TiO}_2$  nanocrystals both after repeated washings

- (19) (a) Boyle, T. J.; Tyner, R. P.; Alam, T. M.; Scott, B. L.; Ziller, J. W.; Potter, B. G., Jr. *J. Am. Chem. Soc.* **1999**, *121*, 12 104. (b) Schubert, U.; Tewinkel, S.; Lamber, R. *Chem. Mater.* **1996**, *8*, 2047. (c) Schubert, U.; Arpac, E.; Glaubitt, W.; Helmerich, A.; Chau, C. *Chem. Mater.* **1992**, *4*, 291. (d) Doeuff, S.; Dromzee, Y.; Taulelle, C.; Sanchez, C. *Inorg. Chem.* **1989**, *28*, 4439. (e) *Processing of Ceramics*; Hubert-Pfalzgraf, L. G., Lee, B. I., Pope, E. J. A., Eds.; Dekker: New York 1995. (f) Chandler, D. C.; Roger, M. J.; Mark, J. *Chem. Rev.* **1993**, *93*, 1205.
- (20) (a) Sasaki, T.; Watanabe, M.; Hashizume, H.; Yamada, H.; Nakazawa, H. *J. Am. Chem. Soc.* **1996**, *118*, 8329. (b) Ohya, T.; Nakayama, A.; Ban, T.; Ohya, Y.; Takahashi, Y. *Chem. Mater.* **2002**, *14*, 3082.
- (21) (a) Gao, W.; Dickinson, L.; Grozinger, C.; Morin, F. G.; Reven, L. *Langmuir* **1996**, *12*, 6429. (b) Guerrero, G.; Mutin, P. H.; Vioux, A. *Chem. Mater.* **2001**, *13*, 4367.
- (22) (a) Hesse, M.; Meier, H.; Zeeh, B. *Spektroskopische Methoden in der Organischen Chemie*; George Thieme Verlag: Stuttgart, New York. (b) Thistlethwaite, P. J.; Hook, M. S. *Langmuir* **2000**, *16*, 4993. (c) Nara, M.; Torii, H.; Tasumi, M. *J. Phys. Chem.* **1996**, *100*, 19 812. (d) Thistlethwaite, P. J.; Gee, M. L.; Wilson, D. *Langmuir* **1996**, *12*, 6487. (e) Nara, M.; Torii, H.; Tasumi, M. *J. Phys. Chem.* **1996**, *100*, 19 812.

(i.e., before the attachment of phosphonic acids) and after surface modification with TDPA (Figure 5b), thus confirming that the removal of the carboxylic ligands from the TiO<sub>2</sub> surface actually occurred during the postsynthesis processing.

Moreover, the expected weak contributions of the  $-\text{CH}_2-$  bending ( $\sim 1450\text{ cm}^{-1}$ ), of the C–O–H bending ( $\sim 1410\text{ cm}^{-1}$ ) and of the C–OH stretching ( $\sim 1280\text{ cm}^{-1}$ ) bands cannot be unambiguously discerned, owing to the possible coincidence of many signals in Figure 5a., and to the poor signal-to-noise ratio in Figure 5b in the same spectral region.

In the fingerprint region (below  $1300\text{ cm}^{-1}$ ), the broadness and the complexity of the peaks make their unique interpretation quite difficult. The P=O stretching<sup>21</sup> centered at  $1226\text{ cm}^{-1}$  in pure TDPA (Figure 5c) is not present in the spectrum of our TDPA-modified TiO<sub>2</sub> sample (Figure 5b). In addition, the narrow bands ascribable to the P–O stretching at 1074, 1010, and  $950\text{ cm}^{-1}$  in TDPA are remarkably broadened and shifted to lower wavenumbers, as inferred from the broad shoulder resulting at around  $1050\text{ cm}^{-1}$  in Figure 5b. Below  $950\text{ cm}^{-1}$ , the characteristic vibrations of the inorganic Ti–O–Ti network in titanium dioxide can be seen in Figure 5a–b.

The disappearance of the P=O stretching and the broadening of the P–O stretching bands have already reported for ZrO<sub>2</sub> and TiO<sub>2</sub> surfaces<sup>21</sup> modified with phosphonic acids and interpreted as evidence for the coordination of all phosphoryl oxygens to surface Lewis acid sites and for the delocalization of electrons. Accordingly, the main bonding mode of phosphonate headgroups to the titania surface is known to involve both tridentate and bidentate attachment (i.e., R–P(OTi)<sub>3</sub> and R–PO(OTi)<sub>2</sub> units, respectively),<sup>21</sup> thus accounting for the strong affinity of phosphonic acids for the TiO<sub>2</sub> surface.

#### 4. Discussion

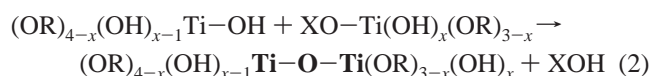
In this report, a novel chemical route in homogeneous solution for well-crystallized anatase TiO<sub>2</sub> nanorods under easily controlled and mild conditions has been presented. The fundamental factors affecting the growth and crystallinity of TiO<sub>2</sub> particles were investigated by simple variation of the synthesis conditions.

Rod formation requires anisotropic crystal growth which is usually realized when the surface free energies of the various crystallographic planes differ significantly. The use of different surface ligands which bind selectively to the respective surface planes has been previously demonstrated as a suitable approach for rod formation in a controlled manner.<sup>1a,4a,5a–b</sup>

In our monosurfactant system (OLEA), the potential for unidirectional growth of TiO<sub>2</sub> particles can be understood as arising from two intrinsic reaction conditions: first, the actual titania molecular precursor is a titanium oxocarboxyalkoxide which likely has some “anisotropic” reactivity; and second, oleic acid may serve as adsorbing-chelating ligand, inhibiting the growth rate along some crystallographic directions. With these underlying prerequisites, the most influential factor in shape control is ultimately provided by the modality of water supply in the reaction mixture. One-dimensional growth can be accentuated by fast hydrolysis (direct injection of large aqueous base volumes) of the precursor, whereas nearly spherical particles are obtained if water is released slowly (from esterification of OLEA and an added alcohol) in the reaction mixture. We will now discuss both issues.

We have employed a modified sol–gel process to synthesize organic-capped TiO<sub>2</sub> nanocrystals at low temperature. The reaction of titanium isopropoxide, TTIP, and water is carried out under the control of the fundamental processes related to the nucleation and growth of titania (see Scheme 1).

Growth of the Ti–O–Ti network is known<sup>15</sup> to proceed through two main steps: first hydrolysis (eq 1) produces unstable hydroxyalkoxides Ti(OH)<sub>x</sub>(OR)<sub>4–x</sub>; then polycondensation reactions (eq 2) follow via ololation or oxolation (i.e., preferential elimination of water or of alcohol, respectively), leading to an extensive Ti–O–Ti network



where R =  $-\text{CH}(\text{CH}_3)_2$ ; X = H, R.

The dehydrative (or dealcoholic) polycondensation reactions (eq 2) need both deprotonation of one  $-\text{OH}$  group and dehydroxylation (or dealkoxylation) of another  $-\text{OH}$  (or  $-\text{OR}$ ) to yield a Ti–O–Ti oxo-species and water (or alcohol). The former process can be accelerated by a base, whereas the latter can be promoted by an acid.<sup>15a,15c</sup>

In most sol–gel preparations, massive precipitation of amorphous TiO<sub>2</sub> is generally accompanied by uncontrolled branching<sup>15c</sup> of the resulting Ti–O–Ti network, since hydrolysis and condensation are very fast and proceed at once. Under these conditions, particle growth is most likely governed by kinetics rather than by thermodynamics,<sup>15b</sup> so that high temperatures and/or additives are required to obtain crystalline material.<sup>15–18</sup>

To exhibit control over the evolution of the oxide structure and morphology under solution-like homogeneous conditions, it is desirable to separate the steps of hydrolysis and condensation even at high concentration of alkoxide and water. The present synthetic approach allows to realize conditions under which hydrolysis of the molecular precursor is slowed, whereas polycondensation is promoted under chemical reversibility to ensure a crystalline product at as low a temperature as  $80\text{ }^\circ\text{C}$ .

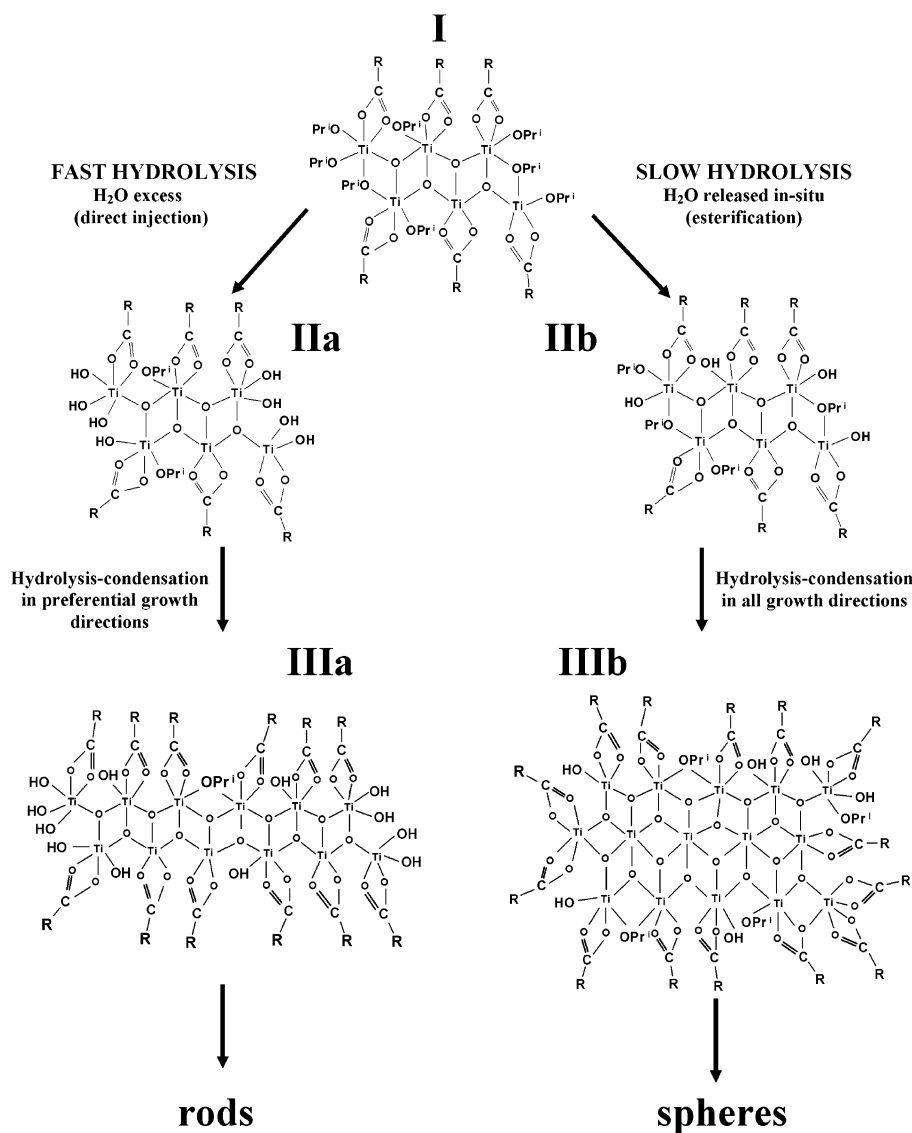
A strategy has been therefore employed to slow the hydrolysis rate, which relies on the use of OLEA both as stabilizing solvent and as chemical modifier of TTIP, ultimately leading to a precursor with a different molecular structure, geometry, and reactivity. Titanium alkoxides are, in fact, known to readily react with carboxylic acids<sup>19</sup> in mild conditions by competitive pathways: substitution (eq 3a), non-hydrolytic condensation and/or elimination of an ester (eq 3b) that generates Ti–O–Ti bonds, or by hydrolysis–condensation (eq 1 and 2) after a slow esterification (eq 4)



Upon modification with carboxylic acids, polynuclear oxocarboxyalkoxides have been reported depending on experimental conditions.<sup>19a,19d–f</sup> These molecular species typically comprise a compact Ti–O–Ti framework of hexa-coordinated Ti atoms,



**Scheme 1.** Hypothesized Mechanism for Anisotropic (route a) and Isotropic (route b) Growth Nanocrystals in Oleic Acid as Pure Solvent ( $-\text{OPr}^i = -\text{CH}(\text{CH}_3)_2$  and  $\text{R} = \text{OLEA Alkyl Chain}$ )



surrounded by a hydrocarbon periphery: thus, they can be thought as actual nanotitania cores protected by carboxylate ligands, these latter having the propensity to bridge metal centers<sup>19f</sup> (Scheme 1, step I). Because of the existence of Ti–O–Ti linkages even before hydrolysis, the modified precursor molecules act as “monomers” for the development of an extended Ti–O–Ti network. A detailed characterization of the actual titanium oxocarboxylalkoxide resulting from the reaction of TTIP and OLEA in our synthesis was beyond the scope of our work; nevertheless, we assumed that the quite general concepts mentioned above may be extended to our case, as experimental evidence is in good agreement with this picture.

As a matter of fact, the growth of the inorganic Ti–O–Ti network in OLEA was affected to a considerable extent. First, the hydrolytic susceptibility of the TTIP:OLEA precursor was significantly decreased with respect to that of the unmodified alkoxide, as no precipitate could be grown in pure OLEA at temperatures lower than 80 °C. In contrast, in the absence of any surfactant and additive, TTIP vigorously reacts with water at low temperatures in organic solvents,<sup>15,17,18</sup> providing precipitation of amorphous  $\text{TiO}_2$ . In our system, heating at  $T > 80$

°C was necessary to force hydrolysis of TTIP–OLEA precursor. The existence of a significant energetic barrier for hydrolysis can be connected with the steric hindrance of the overall TTIP:OLEA precursor structure: carboxylic chains can effectively hinder the attack of water at metal centers, allowing only the most exposed  $-\text{OR}$  groups to be primarily hydrolyzed<sup>19</sup> (Scheme 1, step II).

Second, the modified molecular precursor itself has a potential “anisotropic” reactivity, as the accessibility of  $-\text{OR}$  groups toward water depends on their spatial orientation in the starting oxocarboxylalkoxide. The directions, in which cross-linking of Ti–O–Ti bonds can occur, can thus be limited.<sup>15c,19a</sup> Unidirectional growth of the particles was guaranteed in OLEA at high TTIP concentration when large volumes of water were rapidly injected in a single portion (fast hydrolysis method). In such case, the system is kinetically overdriven by an extremely high monomer concentration in the early growth stages,<sup>1a,5f</sup> the sterically limited exposure of  $-\text{OR}$  moieties in the precursor can ultimately result in a face-dependent surface density of  $-\text{OX}$  ( $\text{X} = \text{R}$  or  $\text{H}$ ) moieties in the growing titania clusters (Scheme 1, step IIa). As a consequence, rather than monomer supply

from the bulk solution, the slow growth step can be some surface process, like incorporation of TiO<sub>2</sub> “building blocks” by means of successive condensations of –OX groups. Anisotropic growth proceeds, as polycondensations are more likely to take place on the –OX moieties-rich planes of the growing titania clusters (Scheme 1, step IIIa).

It has also been suggested<sup>15c</sup> that growth of a network of low dimensionality can be promoted by means of an acid–base pair catalyst, which would somehow increase the overall polycondensation rate (eq 2) without affecting the hydrolysis rate.<sup>15c</sup> In this respect, the salt deriving from the reaction between OLEA and the employed base catalyst could play a role as an acid–base pair catalyst under our synthesis conditions, thus acting as an additional factor accounting for anisotropic growth.

Interestingly, if some conditions that can potentially promote anisotropic growth of the TiO<sub>2</sub> nanocrystals are retarded, the final shape is nearly spherical. For example, at low monomer concentration, Ostwald ripening favors the formation of spherical particles.<sup>1a,5f</sup> A similar situation can actually occur in our system when water is slowly released upon esterification of OLEA and alcohol (slow hydrolysis method): in such case, nearly spherical particles were obtained (Figure 2c and Figure 2e). Anisotropic growth is suppressed as water concentration is always low, especially in the early growth stages when it is consumed as soon as it is produced in-situ (Scheme 1, step II b). The difference in growth rates along the various crystallographic directions cannot be accentuated in this case, as the overall growth rate is slow (Scheme 1, step III b).

The observation that rodlike TiO<sub>2</sub> nanocrystals are mainly formed in a kinetically overdriven growth regime, seems to exclude a structured micellar templating<sup>6a–b,15h</sup> mechanism to account for the diverse growth regimes in pure OLEA.

By comparison, dynamic removal and subsequent restructuring of OLEA molecules on the surface of the growing titania nanocrystals is likely face-selective and accentuated at high growth rates (i.e., at high water and TTIP concentration). This was confirmed by the detection of low aspect ratio elongated particles at low OLEA concentration in OLEA/alkane mixtures. The long-chain carboxylate ligands act as polymerization lockers by capping the surface of the growing titania and stabilizing polar polynuclear oxo-aggregates generated by hydrolysis, thus preventing aggregation and premature precipitation. The introduction of a noncoordinating solvent (like HPD or HXD) strongly destabilizes the growing titania clusters, leading to particles with a broad distribution of aspect ratios and to increased time for full crystallization. A number of surface sites on the growing TiO<sub>2</sub> would be left unprotected by OLEA molecules, thus making OLEA less and less effective in face-selective adsorption with increasing HPD/ HDC fraction (see Figure 3). Accordingly, a tendency to aggregation among particles during the course of the reaction was observed with decreasing OLEA content in the growing mixtures. As a direct consequence, the nanocrystals prepared under these conditions were scarcely soluble in apolar solvents after extraction procedures.

It can also be assumed that OLEA participates in a reversible, dynamic equilibrium on the nanocrystal surface. This assumption is supported by the observation that repeated washing of nanocrystals resulted in TiO<sub>2</sub> nanocrystals which could not be redispersed in apolar solvents, unless addition of fresh OLEA

was carried out. Accordingly, an increase in the temporal stability of organic TiO<sub>2</sub> nanocrystal dispersions was provided by the presence of a little excess of surfactant with respect to the amount necessary for a full surface coverage.

Surface ligand-exchange with OPA or TDPA clearly proved that exceptionally stable colloidal dispersions could be provided upon capping of TiO<sub>2</sub> nanocrystal surface with phosphonic acids. In this case, no excess of stabilizer was required in the bulk organic solution to ensure the colloid stability. The study of the TiO<sub>2</sub> surface by FTIR spectroscopy (Figure 5) demonstrated the feasibility of almost completely removing the carboxylate groups from the TiO<sub>2</sub> surface and subsequently restoring the nanocrystals solubility in organic media by modifying their surface with phosphonic acids.

As described in the Experimental Section, the reverse ligand exchange procedure (i.e., exchange of the phosphonic ligands with OLEA) was unsuccessful: the either OPA- or TDPA-capped nanocrystals retained their solubility in apolar media even after repeated washing. This fact indicated that the attachment of phosphonic acids onto the TiO<sub>2</sub> surface implies a much stronger anchoring than a reversible adsorption, as opposed to the case of OLEA.

Upon ligand exchange, the IR spectra of the capped nanocrystals were dominated by the remarkably modified bands of the phosphonic ligands when compared to the spectra of the free alkyl phosphonic acids. Although a conclusive interpretation of the surface binding sites could not be ruled out, the remarkable changes observed in the P–O stretching region suggested a strong coordination of the phosphonate headgroup to the surface of TiO<sub>2</sub>, in agreement with well-documented data in literature.<sup>21</sup>

The presented results highlight that OLEA, besides being a suitable surfactant for growing TiO<sub>2</sub> nanocrystals under controlled hydrolysis conditions, offers the unique possibility of postsynthesis attaching other functional molecules because of its reversible binding to the titania surface. In this respect, the proposed synthetic approach provides the potential for varying the characteristics of TiO<sub>2</sub> nanocrystals surface by changing the capping ligands in a simple way.

The easy crystallization process in the mild conditions of our work (at as low a temperature as 80 °C) can be attributed to a specific action played by bulky amines and alkylammonium hydroxides in our synthesis. Amines may promote a chemical reversibility in the Ti–O bonding formation: upon attacking the electrophilic Ti center of the alkoxide precursors or of a partially formed titania network, an amine/alkoxy or amine/titanyl exchange<sup>16e</sup> can occur, thus resulting in a Ti–O bond breaking and forming. Defects incorporated in the growing titania network could be erased. This hypothesis is supported by the fact that alkoxy-ligand exchange can occur easily even at nearly room temperature.<sup>16a–c</sup> On the other hand, dissolution-growth<sup>15b</sup> mechanisms for TiO<sub>2</sub> particle growth, similar to Ostwald ripening, have already been suggested to explain the formation of metastable phases (like anatase) upon dissolution of preformed amorphous titania nuclei. Moreover, a recent study on the formation of transparent, aqueous colloidal ammonium titanate<sup>20</sup> solutions has shown that the chemical species deriving from hydrolysis of titanium alkoxides in the presence of bulky alkylamines (or tetraalkylammonium hydroxides) have a flexible structure, easily changeable by reaction with other chelating

ligands. The authors suggest that depolymerization (and thus Ti–O breaking and forming) of hydrous titania to lower condensed and soluble species can easily occur in the early stages of hydrolysis, whereas alkylammonium cations prevent<sup>20,15a</sup> a premature collapse of the growing species into insoluble polymeric structures.

## 5. Conclusions

We have reported a novel and simple wet-chemical synthesis of organic-capped anatase TiO<sub>2</sub> nanorods at as low a temperature as 80 °C. Chemical modification of a titanium alkoxide has been proven to be a rational strategy to tune the reactivity of the precursor toward water to manipulate the nanocrystal's

growth kinetics and achieve shape control over the resulting nanoparticles. Tertiary amines or quaternary ammonium hydroxides have been demonstrated effective catalysts to promote crystallization in mild conditions. The novelty of the present approach when compared to earlier works can be characterized by the large-scale production of oxide nanocrystals to which standard processing of colloidal nanocrystals can be applied. In this respect, the proposed synthetic route provides a unique tool for easily functionalizing the TiO<sub>2</sub> nanocrystals surface with different capping ligands. The obtained titania nanocrystals are highly soluble in apolar solvents and thus available for fundamental studies in homogeneous solutions.

JA036505H